Polymer films on electrodes
Part 29. Electropolymerized poly(7,14-diphenylacenaphtho[1,2-k]fluoranthene): electrochemistry and conductance of a novel electrochromic hydrocarbon ladder polymer film

Maurizio Quinto, Allen J. Bard *

Department of Chemistry and Biochemistry, The University of Texas at Austin, Austin, TX 78712, USA

Dedicated to Fred C. Anson for his distinguished contributions to electrochemistry

Abstract

The electropolymerization of 7,14-diphenylacenaphtho[1,2-k]fluoranthene on a platinum or indium tin oxide (ITO) electrode produces an electroactive film which displays fluorescence and electrochromism. We report a study of the electrochemical properties and other characteristics of this film, such as the resistance dependence by the potential applied to the electrode. In particular, the film showed dramatic changes in the resistance and color as a function of the potential applied to the film because of changes in the electronic state of the polymer. Atomic force microscopy, scanning electrochemical microscopy, and electrochemical quartz crystal microbalance studies were also carried out to characterize the polymer film. © 2001 Elsevier Science B.V. All rights reserved.

Keywords: Polymer films; Electrochromic films; Conductance

1. Introduction

In addition to fundamental interest in the properties of polymer films on electrode surfaces, practical applications, such as electrochromic behavior, have been suggested. These have possible use in displays, smart windows, and other applications where the nature and intensity of the color can be controlled electrically. In general, for practical applications these films should possess high stability under long-term cycling, rapid optical changes with applied electrical signal required to achieve optical tunability, satisfactory color contrast, durability, the processability of the chromogenic materials into suitable forms (conformational coatings, multilayers), and a variety of necessary properties beyond optical tunability (e.g. mechanical strength).

In a previous preliminary study, a new hydrocarbon ladder polymer (PANF), obtained by electropolymerization of 7,14-diphenylacenaphtho[1,2-k]fluoranthene (ANF), showing interesting electrochromic behavior and high stability of the surface layers was described [1]. A ladder polymer is one in which the monomeric units are coupled to one another with two bonds rather than the single bond coupling that characterizes polymers like poly(vinylferrocene) and polypyrrole. To understand better the characteristics of films of PANF and to correlate its redox properties and spectroscopic behavior with molecular structure, a detailed electrochemical study was carried out. We also determined the resistance dependence on the applied electrode potential, surface topography, and film thickness by atomic force microscopy (AFM) and scanning electrochemical microscopy (SECM), and mass changes during electrochemical cycling by electrochemical quartz crystal microbalance (EQCM) measurements. Measurement of the resistance for a film deposited onto an electrode

---

* Corresponding author. Tel.: +1-512-471-3761; fax: +1-512-471-8696.

E-mail address: ajbard@mail.utexas.edu (A.J. Bard).

surface represents an interesting field for a number of purposes, ranging from the anodic dissolution of metals to the study of electrochromic films of indium oxide [2]. In the past, several techniques were used for such resistance measurements, based on discontinuous determinations [3–5], or continuous determinations (impedance measurements via a 90° quadrature signal from a lock-in amplifier [6], SECM inside the film [7], impedance spectroscopy [8], scanning tunneling microscopy [9], and indirect electrochemical measurements [10,11]). In this paper a new and simple method to measure the film resistance as a function of potential was developed. It employed a four microband-electrode array covered by the electrodeposited film. The resistance measurement was performed with a d.c. voltmeter connected with the two central microbands while the potential applied to the external microbands was varied.

2. Experimental

Tetra-n-butylammonium hexafluorophosphate (TBAPF$_6$) (SACHEM, Austin, TX) was recrystallized from EtOH + H$_2$O (4:1) twice and dried at 100°C before use. Benzene (Aldrich, anhydrous) and MeCN (Burdick and Jackson, UV grade) were used as received after being transported unopened into an inert atmosphere drybox (Vacuum Atmospheres). All the other chemicals were used as received. The reference electrode was calibrated versus an SCE by the addition of ferrocene (Fc) as an internal standard taking the formal potential of Fc/Fc$^+$ as 0.424 vs. SCE. All the potentials quoted are referred to the SCE reference electrode. Different working electrodes were used during the electrochemical experiments: Pt disk electrodes (3 mm diameter unless otherwise specified), indium-tin-oxide-coated glass electrodes (ITO, R_s 40 Ω/square, Delta Technologies, MN), and an array of four Pt microelectrodes (IMT, Neuchâtel, Switzerland). The microelectrodes assembled in this array were 1 mm long, 25 μm wide, and 25 μm apart, and they were fabricated on a Si$_3$N$_4$ passivated Si wafer [12]. The completed structures were mounted on a printed circuit board support and wire bonded and all except the array were covered with epoxy encapsulation.

Cyclic voltammograms and electropolymerizations were carried out with a model 660 electrochemical workstation (CH Instruments, Austin, TX). The resistance measurements were carried out by coupling a PAR model 175 universal programmer and a model 173 potentiostat (Princeton Applied Research) with a d.c. voltmeter connected to a computer via a LabView interface.

The experimental setup for SECM measurements has been described previously [13]. Potentiostatic experi-

ments of the polymer-covered substrate were carried out with two different mediators depending on the potentials applied to the substrate, that is, tetrathiafulvalene (TTF) and 7,7′,8,8′-tetracyanoquinodimethane (TCNQ) were used to get approach curves with the substrate at −1.15 and 1.1 V, respectively. Preliminary cyclic voltammetry with these compounds suggested the potentials that should be applied to the tip for the approach curve experiments for the electrode reactions to be diffusion controlled: −0.60 V for TCNQ reduction and 0.05 V for TTF oxidation. The tip was positioned close to the polymeric film in the conductive state ($E_{sub} = 1.1$ V). The electrolyte was MeCN with 0.1 M TBAPF$_6$, and the concentration of the mediator was 5 mM in both cases. The solutions were bubbled with Ar before the SECM experiments, and during the measurements, the cell was maintained under an Ar atmosphere. A model 660 electrochemical workstation (CH Instruments) was employed for the tip characterization in the absence of the polymeric substrate.

Imaging AFM experiments were performed with a Nanoscope III (Digital instruments, Santa Barbara, CA) in air, at room temperature and atmospheric pressure. The images were not digitally filtered. The sample was manually positioned below the tip and maintained perpendicular to the tip and parallel to the tip scan plane through manipulation of the microscope adjustment screws. For a depth profile study and to determine the film thickness with AFM measurements, part of the film was removed from the ITO surface using a razor blade.

The EQCM measurements were performed with a home-built instrument described elsewhere [14]. A simple battery driven TTL oscillator with an optoisolator was used to isolate the ground of the QCM circuit from the potentiostat (PAR 173 and 175). A Philips model PM6681 frequency counter monitored the output of the optoisolator.

2.1. 7,14-Diphenylacenaphtho[1,2-k]fluoranthene

This compound was prepared by a route similar to that previously reported [1]. The cyclopentadienone intermediate was prepared by refluxing 1,3-diphenylacetone (3.72 g, 17.7 mmol) and acenaphthenequinone (3.23 g, 17.7 mmol) in ethanolic KOH for 6 h. The solvent was removed under vacuum, and the residue was dissolved in CH$_2$Cl$_2$ and filtered (the cyclopentadienone can be isolated at this step by addition of pentane to the filtered solution to precipitate the compound; however, isolation is not required for the following preparation). The solvent was removed and acenaphthylene (2.70 g, 17.8 mmol) and xylene (40 ml) were added and the resulting solution was refluxed for

2 days. The solvent was removed by distillation and the residue was placed under vacuum to remove unreacted acenaphthylene. Then DDQ (4.0 g, 18 mmol) and sufficient CH_2Cl_2 to dissolve the residue was added, and the solution was stirred at 45°C for 1 h. The solution was filtered through silica (3 cm) and the solution volume was reduced under vacuum. The product precipitated as yellow crystals, which were isolated by filtration. The supernatant was reduced further and cooled to induce the product to crystallize (5.15 g total, 61%). The compound was recrystallized from toluene before use in the electropolymerization experiments.

2.2. Electropolymerization of 7,14-diphenylacenaphtho[1,2-k]fluoranthene

The solution used for electropolymerization consisted of the monomer in benzene + MeCN (4:1) containing 0.2 M $TBAPF_6$. The monomer shows low solubility in MeCN alone. The concentration of the monomer was typically 2 mM, unless otherwise specified. The electropolymerization was carried out in an electrochemical cell with a quasireference electrode (a Ag wire inside a small fritted glass tube with a MeCN solution containing 0.1 M $TBAPF_6$) and a Pt coil as counter electrode. Unless otherwise specified, care was taken to avoid any oxygen and water dissolution in the cell by preparing the electrolyte solution in a drybox (Vacuum Atmospheres) and using a cell that did not permit any contact of the solution and the electrodes with the atmosphere. Polymer (PANF) was deposited on the working electrode by repeatedly sweeping the potential from 0.0 V to the oxidation peak of the monomer (1.6 V vs. SCE) at a scan rate of 100 mV s^{-1}. The solution became green during the experiments, because of the generation of oligomers [1]. The polymer-coated electrode was washed in MeCN after removal from the electropolymerization cell. The polymer is insoluble in MeCN, so that the polymer film remained intact over a broad range of potentials during the electrochemical experiments in MeCN.

3. Results and discussion

3.1. Electrochemical characterization

The electrochemical process that produces the polymerization is shown in Fig. 1. Molecular orbital calculations reveal that the highest electron density for the compound is located mainly in the central positions (7 and 14) and at the end positions (3, 4, 10 and 11); so reactions of the radical cation of the compound, such as intermolecular coupling, would be expected to occur primarily at these positions. However, substitution of

the central 7 and 14 positions with alkyl or aryl groups prevents reactions at these carbons and directs reactivity of the radical cation toward the ends of the molecule, promoting the linear polymerization via an oxidative coupling route. As shown in a previous paper [1], the cyclic voltammogram of the monomer (Fig. 2) shows two reversible reduction processes (at -1.61 and -2.10 V), and an oxidation wave ($E_{pa} = 1.52$ V) that is chemically irreversible, indicating that the radical cation is not stable and quickly undergoes a following chemical reaction. The separation between the first and second reduction is about 0.5 V; this value is typical for polyaromatic hydrocarbons [15–17]. During the reverse scan, new peaks appear at -1.06 and -1.29 V; these peaks have a lower $E°$ than that of the monomer peaks, demonstrating a more extensive electronic delocalization, and are characterized by a small ΔE_p, which is typical of a solid-state redox process [18].

When the potential of the electrode was cycled between 0 V and the oxidation wave, a broad and reversible pair of waves grew with time and a blue electroactive film deposited on the electrode, as is typically found for the deposition of conducting polymer films on electrodes by oxidation of a monomer, e.g. pyrrole [19]. The films adhered well to platinum or ITO electrodes and appeared homogeneous and transparent. The changes in the coloration during the cyclic voltammetry are indicated in Fig. 3. Electrochemical oxidation in MeCN initiates a rapid color change to blue–green while the first and second reduction waves cause the film to become green and orange respectively. Prepeaks appear at -0.79 and $+0.80$ V; these are labeled I and II, respectively, in Fig. 3. These two peaks correlate with each other as seen in cyclic voltammetric experiments in the range -0.84 to 0.84 V (Fig. 4). In this experiment, a previous reduction of the film was carried out maintaining a potential at -0.9 V for 10 s. During the first cycle (a), no reduction peaks were recorded. In the oxidation zone, a peak at 0.79 V appeared (b), and subsequently, a reduction peak appeared at -0.80 V (c). The same experiment was carried out starting from the oxidation zone, showing no oxidation peaks on the first cycle. The charge involved in the oxidation and reduction processes is the same and the waves are perfectly reproducible. The large separation between these two peaks suggests changes in the film characteristics, in particular a low conductivity of the film over the potential window that encompasses the oxidation and the reduction waves.

3.2. Resistance measurements

To study the film conductivity and its change with potential, resistance measurements during cyclic
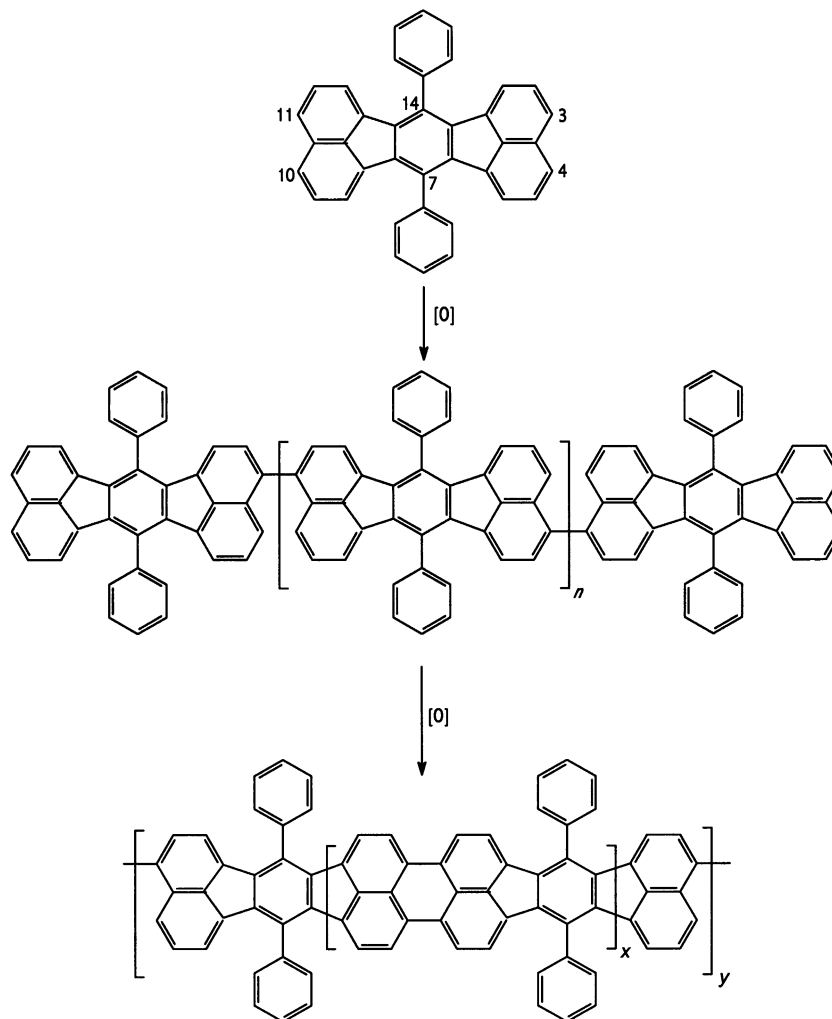
Fig. 1. ANF electropolymerization process.

voltammetry were carried out with an array of four Pt microbands (1 mm long, 25 μm wide, and 25 μm apart; see Fig. 5). The film deposition was effected by connecting the four microbands together and applying the same electrodeposition conditions as used for the single Pt or ITO electrodes. Once the film was prepared, the two central bands were connected to a voltmeter for the resistance measurement, while the external microbands were connected to the potentiostat. The measurements shown in Fig. 6 demonstrate that the neutral form of the polymer has a resistance that is between two and three orders of magnitude greater than the resistance for the oxidized and reduced forms. This parameter in fact increases abruptly as soon as the reduction or the oxidation potential is reached. Furthermore, when the cyclic voltammetry was carried out in the presence of oxygen, the resistance increased during each scan, and after about 10 cycles, the oxidized film was essentially non-conductive. With the oxidized film, no color changes were detected during potential sweeps.

More interesting than the resistance is the resistivity, defined as
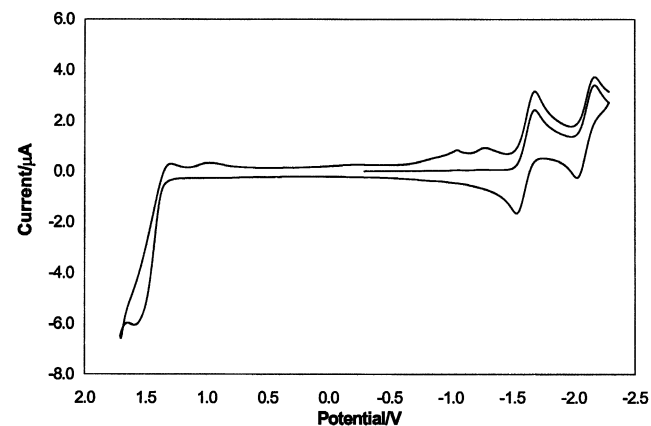
$$\rho = Rs/l$$

Fig. 2. Cyclic voltammetry of 2 mM ANF in benzene + acetonitrile (4:1) + 0.1 M TBAPF$_6$. Scan rate, 0.5 V s^{-1}, initiated from 0 V toward negative potentials. Note that the cathodic current is taken as positive here and in the following.
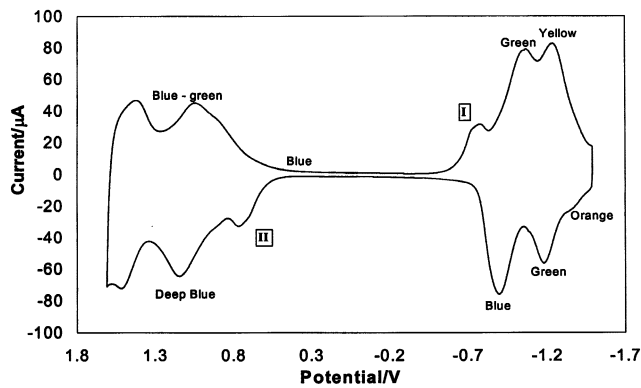
Fig. 3. Cyclic voltammetries of a PANF thin film on an ITO electrode in MeCN + 0.1 M TBAPF$_6$. Scan rate, 200 mV s^{-1}. The colors observed at the different waves are indicated.
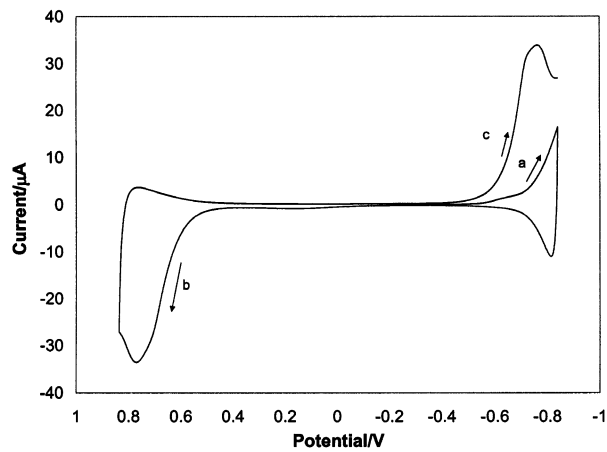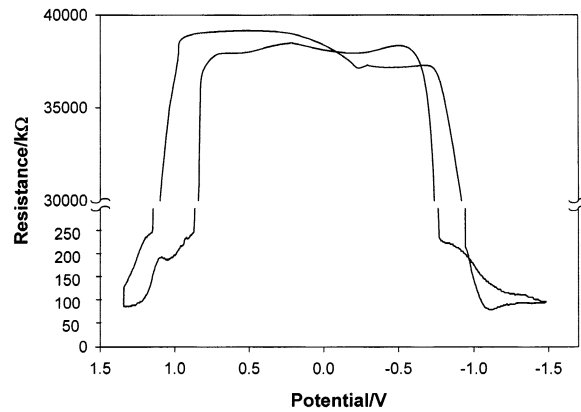

Fig. 6. Resistance dependence of the film during the cyclic voltammetry. Experimental conditions as in Fig. 3, except scan rate of 10 mV s^{-1}. The resistance was measured between the central microbands, while the potential was applied to the external microbands.

Fig. 4. Cyclic voltammetry of a PANF thin film on an ITO electrode in MeCN + 0.1 M TBAPF$_6$, over the range −0.84 to 0.84 V. Scan rate, 200 mV s^{-1}.

where R is the resistance, l the distance between the microbands, and s the area; in this case this value can be reasonably approximated as the thickness of the film multiplied by the length of the microband. To determine the thickness of the film, an AFM depth profile study of the film was carried out. The film morphology (Fig. 7) shows the surface was quite rough, therefore it is possible to calculate only an average thickness; for a film obtained with 50 electropolymerization cycles, this corresponded to 90 ± 18 nm.

An EQCM study revealed that there was a linear relation between the mass deposited on the electrode and the number of cycles used for the electropolymerization (Fig. 8). From the mass of the film determined by the EQCM measurement, 15 µg, and the estimated volume of the film (area, 0.50 cm^2), a film density of 3.3 ± 0.4 g cm^{-3} was estimated. From these data, the resistivity calculated for the film obtained under these conditions ranged from a minimum value of 28 ± 5

Fig. 5. Configuration of PANF on a microband array for the measurement of the resistance as a function of the applied potential.

$\Omega \cdot \text{cm}$ to a maximum of $1.3 \pm 0.3 \times 10^3$ $\Omega \cdot \text{cm}$. Furthermore, from the results in Fig. 3 it is possible to determine the charge (and thus the number of electrons) involved in the redox processes, while the number of monomeric units in the film can be calculated from the mass obtained by EQCM. From these results, the average number of the electrons involved in the two reduc-
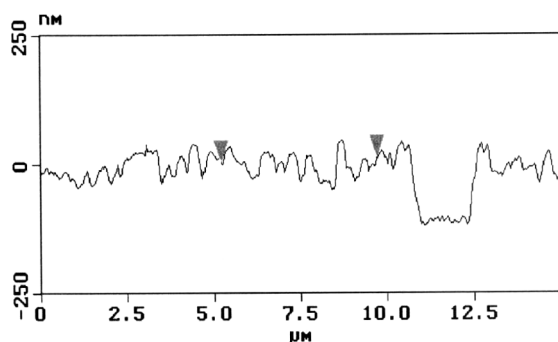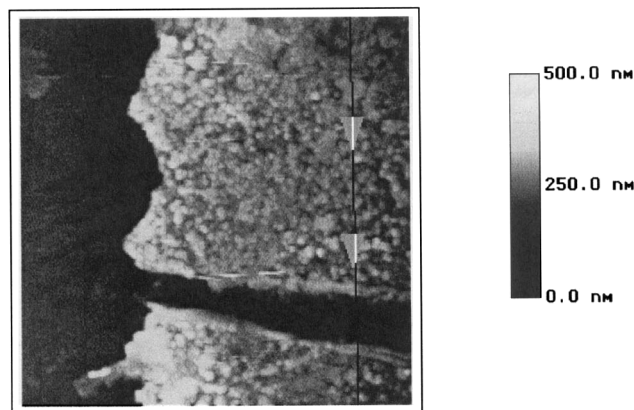

Fig. 7. AFM image of a PANF film (right side) on an ITO surface. The ITO surface is clearly visible on the left side and also through a scratch made in the film with a razor blade. Electropolymerization was carried out as described in the text. Number of cycles 50. Lower plot shows a topographical trace across the film and scratch.
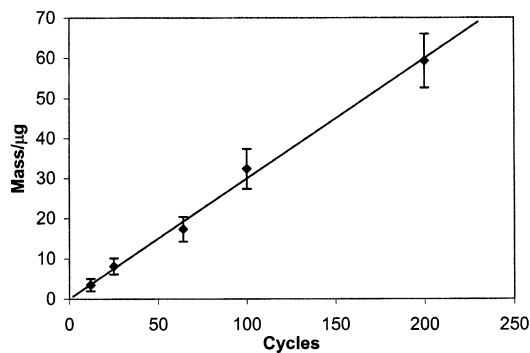

Fig. 8. Relation between the mass deposited on the electrode, as measured by EQCM, and the number of cycles used for the electro-polymerization. The horizontal bars represent the standard error deviation measured on four different experiments.

tion peaks in Fig. 3 is 2.2 ± 0.3, showing that the reduction involves not only the units at the electrode surface but the entire structure of the film.

3.3. SECM studies

The conductivity properties were also investigated by SECM. Previous papers [7,20,21] showed the usefulness of this technique in the study of the transition between the insulating and conductive states of electronically conducting polymers. In general, conductive polymers allowed the regeneration of a mediator species produced at a tip (positive feedback) at the polymer | solution interface, while a non-conductive film produced a negative feedback, that is, a decrease in the tip current as it approached the film | solution interface. To observe negative feedback, it is also necessary that the film is not permeable to the redox species in solution. A small, but finite, film permeability results in a different approach curve with the negative feedback being less pronounced than that obtained with an insulating substrate. Schematic views of the processes involved in the SECM experiments are shown in Fig. 9. The left side of this figure shows the process when the applied potential causes reduction of the PANF film. In this case, the mediator used is TTF. On the right, the figure shows the process when the film is in the oxidized form. TCNQ is used as the mediator in this case and is reduced at the tip. Both cases produce a positive feedback (Fig. 10b and c), while at 0.0 V the film is not conductive (Fig. 10d). Fig. 10 also shows limiting cases: a positive feedback approach SECM curve on a bare Pt surface and negative feedback obtained with a Teflon surface.

The steady-state behavior of the film can be rationalized by the model proposed by Savéant [22] and used by Tsionky et al. [23] in SECM studies. The current across the film | solution interface in an SECM experiment [23,24], as measured by the feedback current at the tip, is affected by four factors: diffusion of the mediator between the tip and polymer surface, electron transfer (ET) at the polymer | liquid interface, charge transport across the polymer film, and ET between the underlying metal and the polymer film (see Fig. 9). In a similar approach to the treatment of ET across a liquid | liquid interface [25,26], one can treat the rates of a number of processes that occur in a serial fashion as a sum of kinetic parameters, represented as currents. The total current across a conductive polymer | liquid interface i_P can therefore be written as:

$$\frac{1}{i_P} = \frac{1}{i_T^c} + \frac{1}{i'_{ET}} + \frac{1}{i_{pol}} + \frac{1}{i''_{ET}}$$

where i_T^c, i'_{ET}, i_{pol} and i''_{ET}, represent respectively the tip current due to the diffusion of the redox mediator, the current due to the ET at the conductive polymer | liquid
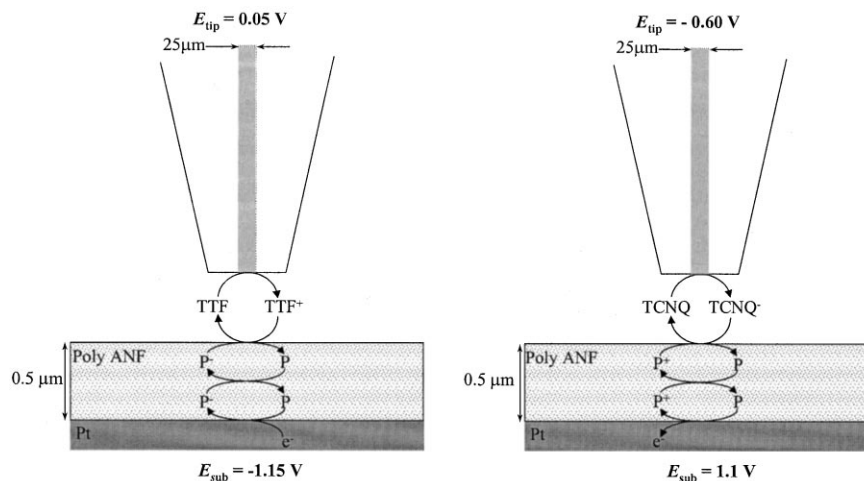
Fig. 9. Schematic of the processes involved in an SECM experiment with the PANF substrate at two different potentials and with the two redox mediators TTF and TCNQ; the experimental results of the two processes are reported in Fig. 10, curves b and c, respectively.

interface, the current due to the charge transport across the polymeric film, and the current for ET at the polymer | metal interface. Because ET is probably fast at the underlying metal | conductive polymer interface, under conditions where there is mediator generation, i''_{ET} is not rate determining in the overall process and can be considered negligible. Contributions for the ET process can be divided into two categories: the diffusion controlled redox mediator generation ($1/i^c_T$), and the ET at and across the polymeric film ($1/i'_{ET} + 1/i_{pol} = 1/i_{eff}$). Diffusive control is obtained for a very thin polymeric film or for a low concentration of redox mediator. On the other hand, a thicker film and a high concentration of redox couple will lead to charge-transfer control. In the present case, we cannot easily separate the factors i'_{ET} and i_{pol}, since changing the potential affects both film resistivity and the ET rate at the film | solution interface. We can, however, use SECM to determine an effective heterogeneous rate constant, k_{eff}, based on the sensitivity of the feedback current to the rate of the overall heterogeneous reactions [27]. From the SECM feedback current–distance curves, it is possible to extract a first-order effective heterogeneous constant fitting the experimental results with the analytical approximation found for these processes [25,26]. The dependence of k_{eff} on the potential applied to the PANF film is strictly correlated to the conductivity properties of the film. When the film is in the more conductive forms ($E_{pol} = -1.15$ V and 1.10 V) the k_{eff} values are relatively high (0.015 and 0.0235 cm s^{-1} respectively) compared to the k_{eff} when the film is not conductive (0.0 V, $k_{eff} = 0.0017$ cm s^{-1}). These values can be represented as characteristic currents, i_{eff}, with the equation

$$i_{eff} = nFAc_M k_{eff}$$

where c_M is the concentration of monomer, 7×10^{-3} mol cm^{-3}, and A is the area below the tip, 5×10^{-6}

cm^2. This yields i_{eff} values in the conducting and resistive regimes of 6×10^{-5} and 6×10^{-6} A, respectively. The ratio of i_{eff} values is somewhat smaller than that predicted from the resistivities, assuming that the rate-determining step is charge transfer through the polymer. However, the film in its resistive form is somewhat permeable to diffusion of tip-generated species and this contributes to the feedback current.

3.4. Permeability experiments

To investigate the permeability of the film in its neutral form, cyclic voltammograms with TTF in solution were taken at the Pt electrode before and after deposition of PANF. The results are shown in Fig. 11. Some permeability was found with this mediator and
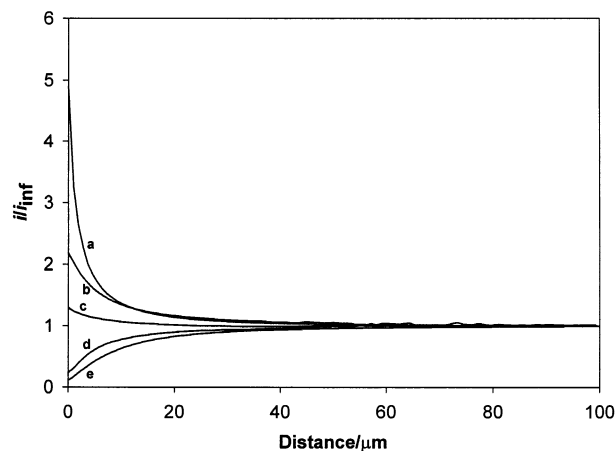

Fig. 10. SECM tip ($a = 12.5$ μm) approach curves with 5 mM TTF (curves a, c, d, e) and 5 mM TCNQ (curve b) as redox mediators on (a) platinum surface; (b, c, and d) PANF at 1.10, -1.15 and 0.0 V, respectively, and (e) Teflon surface. Tip potential, 0.05 V for curves a, c, d, and e and -0.60 V for curve b.
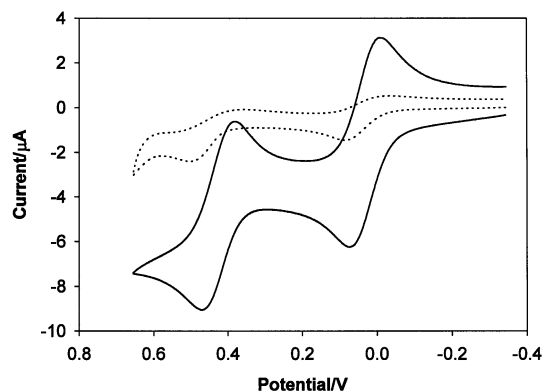
Fig. 11. Cyclic voltammograms of 5 mM TTF in MeCN, 0.1 M TBAPF$_6$ on bare a Pt electrode (diameter, 1 mm) (solid line) and PANF modified electrode (50 cycles) (dashed line).

the shape of the voltammogram is consistent with an array of ultramicroelectrodes, suggesting the presence of pinholes or channels through the polymer film to the substrate. Indeed an optical microscopic examination of this film showed a rough surface with separated small (on the order of tenths of micrometers) zones barely covered or open to the substrate.

4. Conclusions

A study of a poly(7,14 diphenylacenaphtho[1,2-*k*]-fluoranthene) film electrodeposited as a film on Pt or ITO surfaces shows interesting properties. These include changes in film color and in resistance (over two to three orders of magnitude) by varying the potential of the working electrode. The film characterization was carried out by electrochemical, AFM, SECM, EQCM and resistance measurements.

Acknowledgements

References

[1] J.D. Debad, A.J. Bard, J. Am. Chem. Soc. 120 (1998) 2476.
[2] R.L. Deutscher, S. Fletcher, J.A. Hamilton, Electrochim. Acta 5 (1986) 585.
[3] R. John, A. Talaic, G.G. Wallace, J. Electroanal. Chem. 319 (1991) 365.
[4] R. Bezman, Anal. Chem. 44 (1972) 1781.
[5] J.D. McIntyre, W.F. Peck, J. Electrochem. Soc. 117 (1970) 747.
[6] R.A. Bull, F.-R.F. Fan, A.J. Bard, J. Electrochem. Soc. 129 (1982) 1011.
[7] F.-R.F. Fan, M.V. Mirkin, A.J. Bard, J. Phys. Chem. 98 (1994) 1475.
[8] P.G. Pickup, J. Chem. Soc., Faraday Trans. 86 (1990) 3631.
[9] H. Yang, F.-R.F. Fan, S.-L. Yau, A.J. Bard, J. Electrochem. Soc. 139 (1992) 2183.
[10] G.P. Kittlesen, H.S. White, M.S. Wrighton, J. Am. Chem. Soc. 106 (1984) 7389.
[11] E.W. Paul, P.A. Ricco, M.S. Wrighton, J. Phys. Chem. 89 (1985) 1441.
[12] D.J. Strike, A. Hengstenberg, M. Quinto, C. Kurzawa, M. Koudelka-Hep, W. Schuhmann, Mikrochim. Acta 131 (1999) 47.
[13] D. Wipf, A.J. Bard, J. Electrochem. Soc. 138 (1991) 469.
[14] D.A. Cliffel, A.J. Bard, Anal. Chem. 70 (1998) 1993.
[15] M.E. Peover, in: A.J. Bard. (Ed.), Electroanalytical Chemistry, vol. 2, Marcel Dekker, New York, 1967, p. 1.
[16] T. Saji, S. Aoyagui, J. Electroanal. Chem. 144 (1983) 143.
[17] A.J. Bard, Pure Appl. Chem. 25 (1971) 379.
[18] J.D. Debad, J.C. Morris, V. Lynch, P. Magnus, A.J. Bard, J. Am. Chem. Soc. 118 (1996) 2734.
[19] D. Centonze, A. Guerrieri, C. Malitesta, F. Palmisano, P.G. Zambonin, Fresenius J. Anal. Chem. 342 (1992) 729.
[20] M. Tsionsky, A.J. Bard, Chem. Mater. 10 (1998) 2120.
[21] J. Kwak, C. Lee, A.J. Bard, J. Electrochem. Soc. 5 (1990) 1481.
[22] C.P. Andrieux, J.-M. Savéant, in: R.W. Murray (Ed.), Molecular Design of Electrode Surfaces, vol. 22, Wiley, New York, 1992, p. 333.
[23] M. Tsionsky, A.J. Bard, D. Dini, F. Deker, Chem. Mater. 10 (1998) 2120.
[24] A.J. Bard, F.-R.F. Fan, M.V. Mirkin, in: A.J. Bard (Ed.), Electroanalytical Chemistry, vol. 18, Marcel Dekker, New York, 1994, p. 243.
[25] C. Wei, A.J. Bard, M.V. Mirkin, J. Phys. Chem. 99 (1995) 16033.
[26] M. Tsionsky, A.J. Bard, M.V. Mirkin, J. Am. Chem. Soc. 119 (1997) 10785.
[27] M. Tsionsky, A.J. Bard, M.V. Mirkin, J. Phys. Chem. 100 (1996) 17881.